

# Chemistry Letters

<http://www.csj.jp/journals/chem-lett/>

Vol.33 No.4  
April, 2004

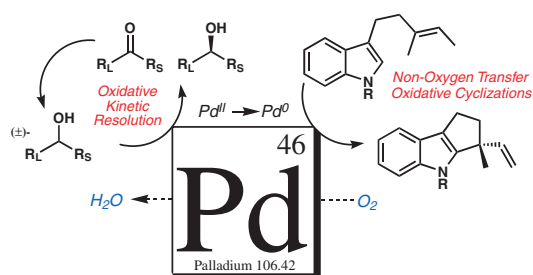
CMLTAG  
ISSN 0366-7022

Copyright © 2004 The Chemical Society of Japan

## Highlight Review

- 362 **Palladium Catalyzed Aerobic Dehydrogenation: From Alcohols to Indoles and Asymmetric Catalysis**

Brian M. Stoltz

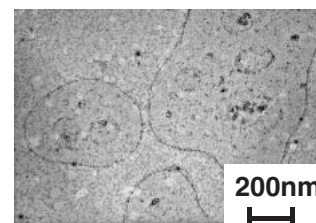


Catalytic aerobic dehydrogenation of organic substrates is going through a Renaissance. Recent advances in this area have led to the discovery of palladium-catalyzed alcohol dehydrogenations and oxidative hetero- and carbocyclizations. The development of asymmetric catalytic dehydrogenations is the latest advance in a long line of catalytic asymmetric oxidation reactions.

## Letter

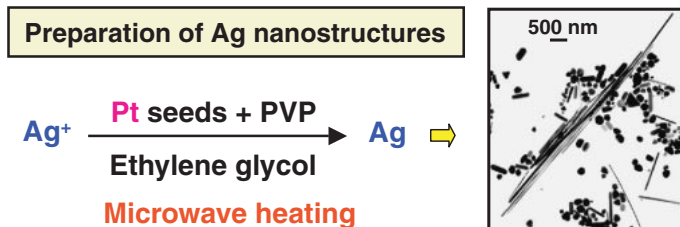
- 368 **Loop Formation of Au Nanoparticles Adsorbed on Langmuir Monolayers**

A Hybrid monolayer of a cationic amphiphile and Au nanoparticles at the air-water interface showed loop structure of the nanoparticles. The loops were 0.1–1  $\mu\text{m}$  in size with a width of around 5 nm, and consisted of the single particle strings.



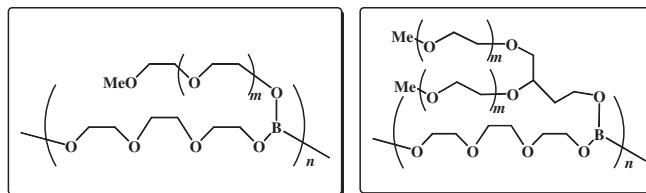
Takeshi Kawai and Tomoyuki Watanabe

- 370 **Syntheses of Silver Nanofilms, Nanorods, and Nanowires by a Microwave-polyol Method in the Presence of Pt Seeds and Polyvinylpyrrolidone**



Masaharu Tsuji, Yuki Nishizawa, Masayuki Hashimoto, and Takeshi Tsuji

- 372 **Preparation of Comb-like Organoboron Polymer Electrolyte without Generation of Salt**



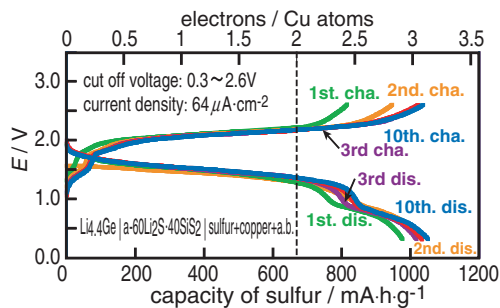
Noriyoshi Matsumi, Tomonobu Mizumo, and Hiroyuki Ohno

- 374 **Synthesis of SBA-1 Mesoporous Silica Crystals with Tunable Pore Size Using Sodium Silicate and Alkyltrimethylammonium Surfactants**



Surfactant chain-length dependence of the SBA-1 mesoporous silica crystal.

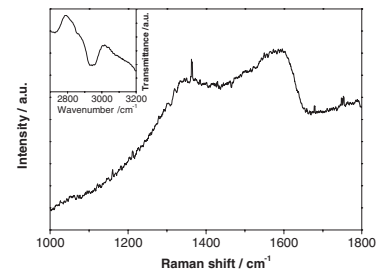
- 376 **An All-solid-state Lithium Battery with Sulfur as Positive Electrode Materials**



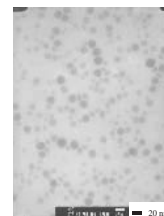
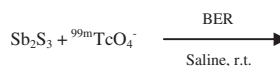
Nobuya Machida and Toshihiko Shigematsu

- 378 **Deposition of Nanostructured Diamond-like Carbon Films on Al Substrate by Facile Electrochemical Route**

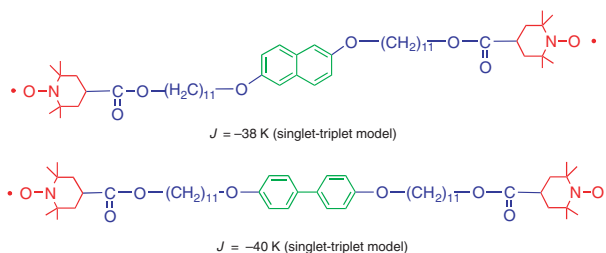
A shoulder peak at  $1355\text{ cm}^{-1}$  and a broad peak at  $1560\text{--}1600\text{ cm}^{-1}$ , identified with the so-called Raman D and G bands, respectively, indicate that the films deposited on Al substrate by electrolysis of dimethylsulfoxide (DMSO) at 150 V are typical DLC films.



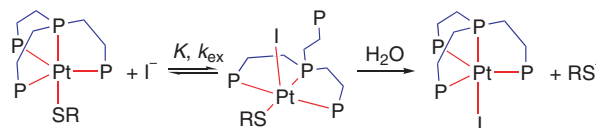
He-qing Jiang, Li-na Huang, Zhi-jun Zhang, Tao Xu, and Wei-min Liu

380 **A Facile and Novel Route to  $^{99m}\text{Tc}$ -labeled Antimony Sulfide Nanocolloid**TEM image of  $^{99m}\text{Tc}$ - $\text{Sb}_2\text{S}_3$  nanocolloid

Sang Hyun Park, Sang Mu Choi, Hui Jeong Gwon, and Kyung Bae Park

382 **Structures and Magnetic Properties of Organic Biradical Compounds with an Aromatic Core and Long Alkyl Groups**

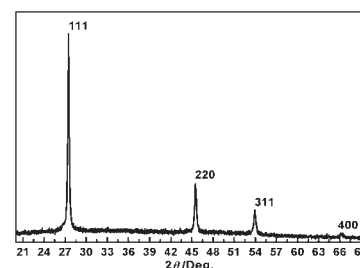
Takamitsu Amano, Hiroki Akutsu, Jun-ichi Yamada, and Shin'ichi Nakatsuji

384 **Rapid Equilibrium between Trigonal-bipyramidal and Square-pyramidal Geometries of 1-Popanethiolato Platinum(II) Complex with Tris[2-(diphenylphosphino)ethyl]phosphine**

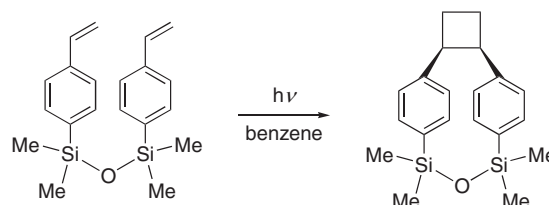
Sen-ichi Aizawa and Tadashi Kobayashi

386 **GaAs Nanocrystals via Hydrothermal Redox Reaction**

Gallium arsenide nanocrystals of 35 nm in size were synthesized via hydrothermal redox reaction of metal gallium with  $\text{As}_2\text{O}_3$  and following annealing.



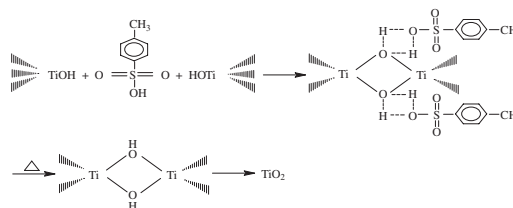
Shuo Wei, Jun Lu, Weichao Yu, Houbo Zhang, and Yitai Qian

388 **Intramolecular  $(2\pi + 2\pi)$  Photocycloaddition of Styrenes Tethered by Siloxanes**

Hajime Maeda, Hiroaki Yagi, and Kazuhiko Mizuno

390 **Preparation of Controllable Crystalline Nano-TiO<sub>2</sub> by Homogeneous Hydrolysis**

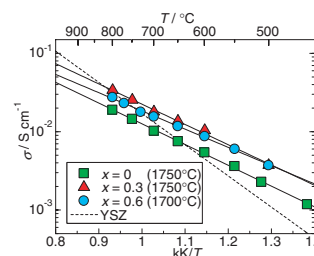
Controllable crystalline nano-TiO<sub>2</sub> was prepared by homogeneous hydrolysis with toluene-p-sulfonic acid, where the mechanism was shown.



Wei Liu, Ai-Ping Chen, Jia-Ping Lin, Zi-Ming Dai, Wei Qiu, Wei Liu, Meng-Qin Zhu, and Shouji Usuda

392 **High Oxide Ion Conductivity in Mg-Doped La<sub>10</sub>Si<sub>6</sub>O<sub>27</sub> with Apatite-type Structure**

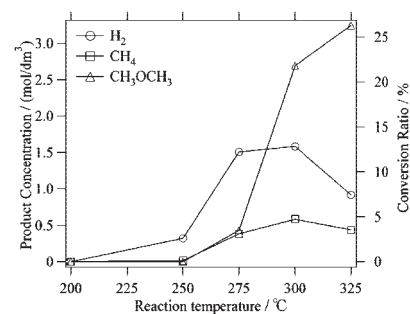
Mg doping increases the ionic conductivity of apatite-type La<sub>10</sub>Si<sub>6</sub>O<sub>27</sub>.



Hideki Yoshioka

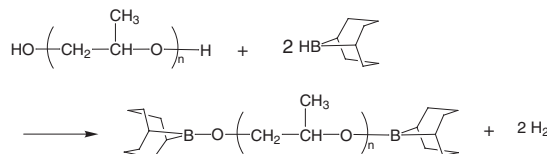
394 **Synthesis of Dimethyl Ether from Supercritical Methanol in the Presence of Aluminum**

Supercritical methanol is treated above 300 °C with aluminum metal to produce dimethyl ether.



Yuma Usui, Chihiro Wakai, Nobuyuki Matubayasi, and Masaru Nakahara

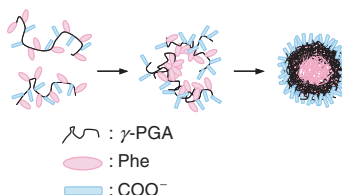
396 **Facile Preparation of Anion Trapping Polymer Electrolytes by Reaction between 9-Borabicyclo[3.3.1]nonane (9-BBN) and Poly(propylene oxide)**



Tomonobu Mizumo, Kenji Sakamoto, Noriyoshi Matsumi, and Hiroyuki Ohno

398 **Stably-dispersed and Surface-functional Bionanoparticles Prepared by Self-assembling Amphipathic Polymers of Hydrophilic Poly( $\gamma$ -glutamic acid) Bearing Hydrophobic Amino Acids**

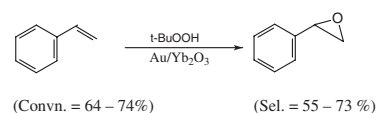
Surface-functional bionanoparticles were prepared by self-assembling amphipathic poly( $\gamma$ -glutamic acid) derivatives with a hydrophilic backbone and hydrophobic phenylalanine and leucine side groups. Poly( $\gamma$ -glutamic acid) bearing phenylalanine nanospheres exhibited excellent water-dispersibility, surface functionality and appropriate size (200 nm) for medical use. Additive PEG conjugation assisted nanoparticle formation of leucine-grafted poly( $\gamma$ -glutamic acid).



Michiya Matsusaki, Ken-ichiro Hiwatari, Mariko Higashi, Tatsuo Kaneko, and Mitsuru Akashi

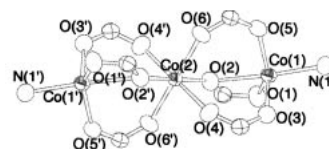
400 **Epoxidation of Styrene by *t*-Butyl Hydroperoxide over Gold Supported on  $\text{Yb}_2\text{O}_3$  and Other Rare Earth Oxides**

Gold nanoparticles deposited [by homogeneous deposition-precipitation (HDP) using urea] on  $\text{Yb}_2\text{O}_3$  and other rare-earth oxides (viz.  $\text{Sm}_2\text{O}_3$ ,  $\text{Eu}_2\text{O}_3$ , and  $\text{Tb}_2\text{O}_3$ ) are novel highly active/selective and reusable catalysts for the selective epoxidation of styrene to styrene oxide by anhydrous or aqueous *t*-butyl hydroperoxide.



N. S. Patil, B. S. Uphade, P. Jana, S. K. Bhargava, and V. R. Choudhary

402 **Structures and Magnetic Properties of a New Cobalt(II) Linear Trimer with Phenylcinamic Acid**

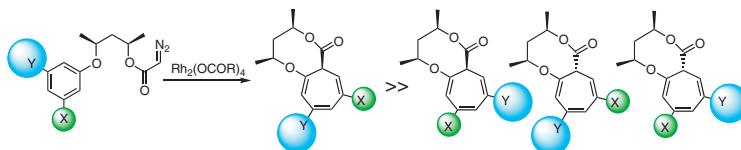


$$J_{\text{Ferro}} = 12 \text{ cm}^{-1} (\text{Co}(1) - \text{Co}(2), \text{Co}(1)' - \text{Co}(2))$$

$$J'_{\text{Ferro}} = 1.4 \text{ cm}^{-1} (\text{nearest neighbor trimer})$$

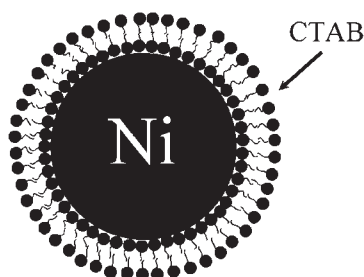
Yoshimi Oka and Katsuya Inoue

404 **Regioselective Formation of Optically Active Cycloheptatrienes by Chiral Tethered Büchner Reaction**



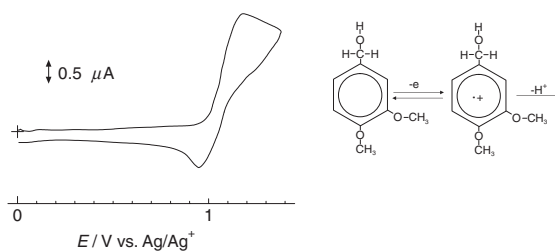
Takashi Sugimura, Naoko Ohuchi, Masami Kagawa, Kazutake Hagiya, and Tadashi Okuyama

406 **Synthesis and Stabilization of Ni Nanoparticles in a Pure Aqueous CTAB Solution**



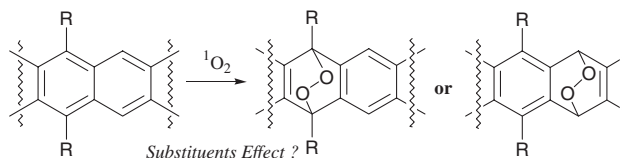
Szu-Han Wu and Dong-Hwang Chen

408 **Lifetime of Veratryl Alcohol Radical Cation Electrogenerated in Acetonitrile**



Shin-ya Kishioka and Akifumi Yamada

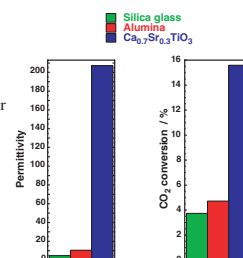
## 410 Substituent Effect on Regioselectivity in Oxygenation of Multisubstituted Acenes



Xin Zhou, Masanori Kitamura, Baojian Shen, Kiyohiko Nakajima, and Tamotsu Takahashi

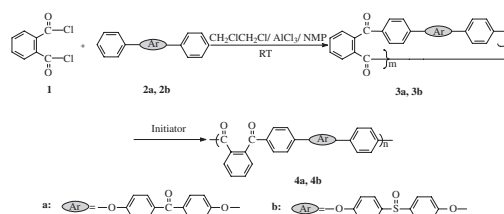
412 Decomposition of Carbon Dioxide by the Dielectric Barrier Discharge (DBD) Plasma Using  $\text{Ca}_{0.7}\text{Sr}_{0.3}\text{TiO}_3$  Barrier

There was no virtual difference on  $\text{CO}_2$  conversion by dielectric barrier discharge (DBD) plasma using silica glass or alumina as the dielectric barriers, however, the conversion was much higher using  $\text{Ca}_{0.7}\text{Sr}_{0.3}\text{TiO}_3$ , which fabricated by liquid phase sintering at  $1200\text{ }^\circ\text{C}$  for 2 h adding  $\text{Li}_2\text{Si}_2\text{O}_5$  (melting temperature ca.  $1030\text{ }^\circ\text{C}$ ) additive. The results suggested that the reactivity of  $\text{CO}_2$  was significantly improved by increasing the permittivity of dielectric barrier material.



Ruixing Li, Qing Tang, Shu Yin, Yukishige Yamaguchi, and Tsugio Sato

## 414 Synthesis of Macrocylic Arylene Ketone Oligomers Containing the Phthaloyl Moiety by Friedel–Crafts Acylation Reaction

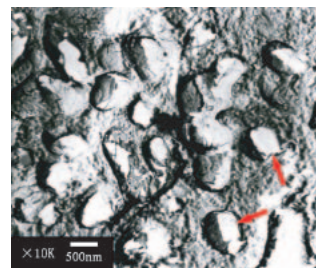


Synthesis and ring-opening polymerization of macrocyclic arylene ketone oligomers

Qingzhong Guo, Shuqin Bo, and Tianlu Chen

## 416 The Studies on the Aqueous Dispersed Particles Formed from Monoolein/Monopalmitin/Water Mixture

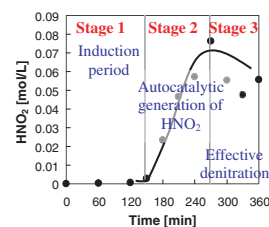
Cubic particles were formed when monoolein/monopalmitin mixture was dispersed in 5–2000 times excess water by vortexing.



Zhining Wang, Joom Y. Um, Liqiang Zheng, and Ganzuo Li

## 418 Efficient Catalytic Reduction of Concentrated Nitric Acid on the Adsorption Sites of Activated Carbon

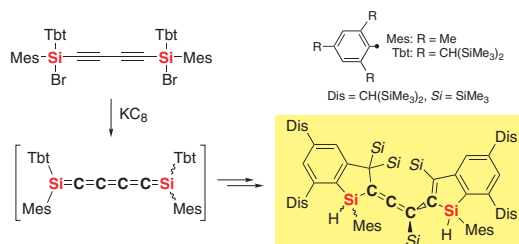
Chemical denitration of concentrated nitric acid by formic acid at low temperature (325 K) was found to occur through 3 stages: (1) induction period, in which the concentration of one of the reaction intermediates,  $\text{HNO}_2$ , increase up to ca.  $0.005\text{ mol/L}$ , (2) autocatalytic formation of  $\text{HNO}_2$  up to  $0.07\text{ mol/L}$ , and (3) effective denitration starts by the formation of gaseous reaction products ( $\text{NO}$ ,  $\text{N}_2\text{O}$ ,  $\text{NO}_2$ , and  $\text{CO}_2$ ). The adsorption site of active carbon was found to have a catalytic effect in the first stage. By addition of active carbon ( $10\text{ g/L}$ ), the induction period of chemical denitration was practically suppressed.



Akane Miyazaki, Kazumasa Shibasaki, Yoshio Nakano, Mitsuteru Ogawa, and Ioan Balint

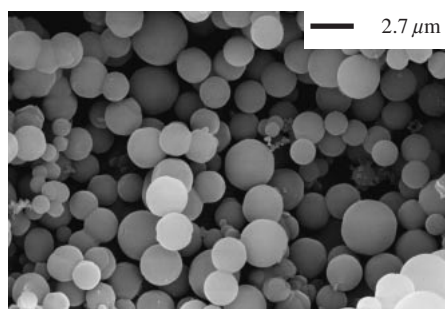
420 **Generation of 1,6-Disilahexapentaene in the Reduction of an Overcrowded Bis(bromodiaryl)butadiyne Leading to the Unexpected Formation of 2-Allenyl-1-benzosilole**

Yoshiyuki Mizuhata, Nobuhiro Takeda, Takahiro Sasamori, and Norihiro Tokitoh



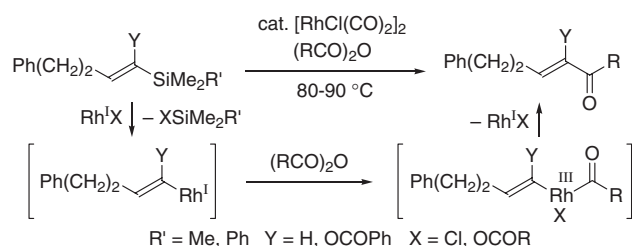
422 **Morphology Control of Organic-Inorganic Hybrid Mesoporous Silica by Microwave Heating**

Dong-Jun Kim, Jin-Seong Chung, Wha-Seung Ahn, Gyoung-Won Kang, and Won-Jo Cheong



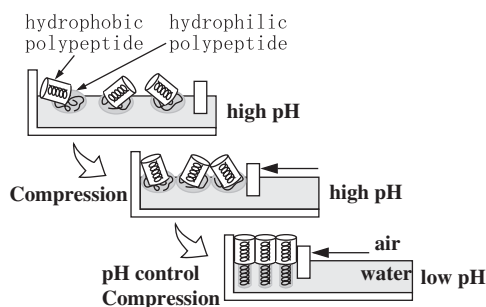
424 **Rhodium-Catalyzed Acylation of Vinylsilanes with Acid Anhydrides: Application to the Transformation of  $\alpha$ -Acyloxy Vinylsilanes to Unsymmetrical 1,2-Diketones**

Motoki Yamane, Kazuyoshi Uera, and Koichi Narasaka



426 **Molecular Orientation Control in Amphiphilic  $\alpha$ -Helical Copolypeptide Monolayer at Air/Water Interface**

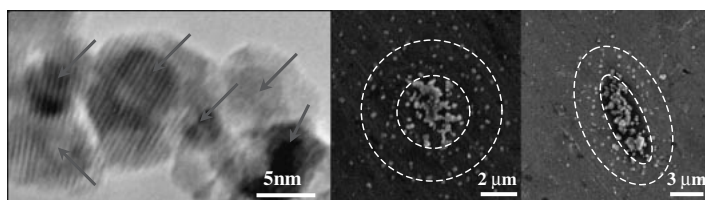
Hidenori Yokoi and Takatoshi Kinoshita



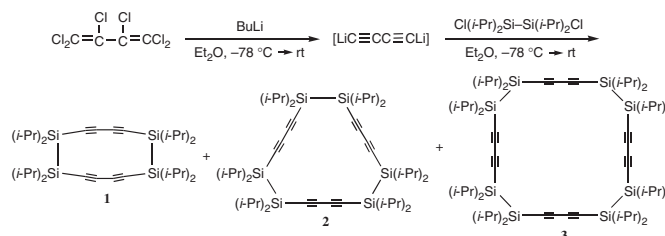
428 **Magnetic Trapping of  $\text{Co}_{\text{core}}\text{CoO}_{\text{shell}}$  Nanoparticles Produced by Gas Phase Reaction**

Seung H. Huh and Atsushi Nakajima

Magnetic trapping of the two kinds of  $\text{Co}_{\text{core}}\text{CoO}_{\text{shell}}$  nanoparticles.

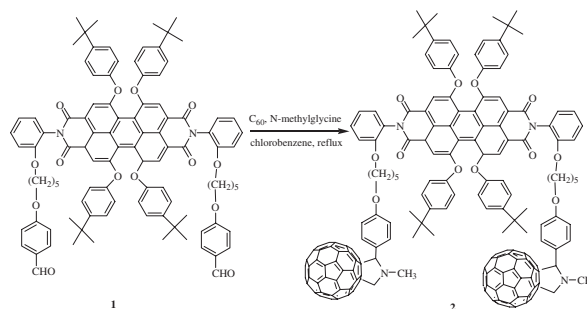


430 **The Cyclo[(disilanylene)(butadiyne)]s**  
 $[(i\text{-Pr})_2\text{Si}(i\text{-Pr})_2\text{SiC}\equiv\text{CC}\equiv\text{C}]_n$  ( $n = 2\text{--}4$ )



Keisuke Negishi, Masafumi Unno, and Hideyuki Matsumoto

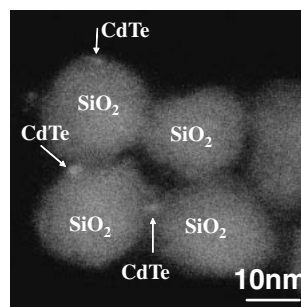
432 **Novel Soluble and Thermally Stable Perylene Dye with Two [60] Fullerene Units**



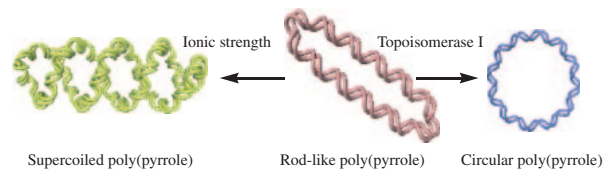
Jianli Hua, Fanshun Meng, Fang Ding, and He Tian

434 **Formation of Luminescent CdTe-Silica Nanoparticles through an Inverse Microemulsion Technique**

S. Tamil Selvan, Chunliang Li, Masanori Ando, and Norio Murase

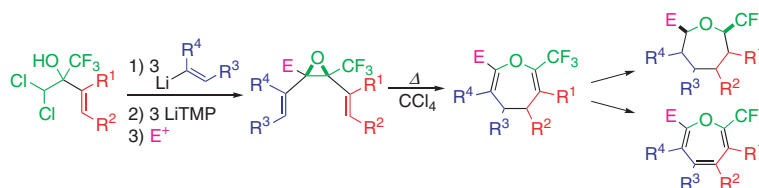


436 **Higher-order Conformations of DNA Are Useful as Templates to Create Various Superstructural Poly(pyrrole) Morphologies**



Ah-Hyun Bae, Tsukasa Hatano, Munenori Numata, Masayuki Takeuchi, and Seiji Shinkai

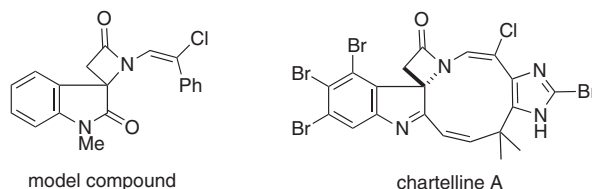
438 **A Facile Approach to 2-CF<sub>3</sub>-Substituted Seven-membered Oxacycles via Stereoselective Preparation and Cope Rearrangement of 2-CF<sub>3</sub>-cis-2,3-Bis(alkenyl)oxiranes**



Masaki Shimizu, Takuya Fujimoto, Xinyu Liu, and Tamejiro Hiyama

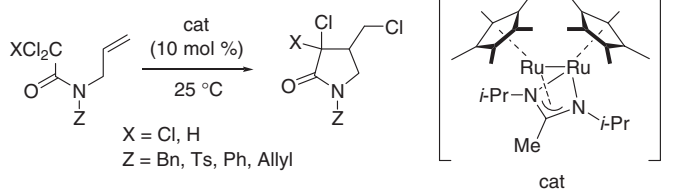


440 **Synthesis of Model Compound Containing an Indole Spiro- $\beta$ -lactam Moiety with Vinylchloride in Chartellines**



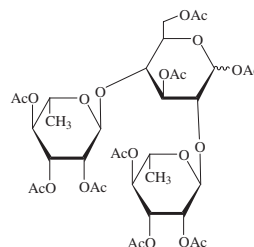
Toshio Nishikawa, Shigeo Kajii, and Minoru Isobe

442 **A Cationic Diruthenium Amidinate,  $[(\eta^5\text{-C}_5\text{Me}_5)\text{Ru}(\mu_2\text{-}i\text{-PrN}=\text{C}(\text{Me})\text{Ni-Pr})\text{Ru}(\eta^5\text{-C}_5\text{Me}_5)]^+$ , as an Efficient Catalyst for the Atom-Transfer Radical Reactions**



Yukihiro Motoyama, Mitsuru Gondo, Satoshi Masuda, Yuya Iwashita, and Hideo Nagashima

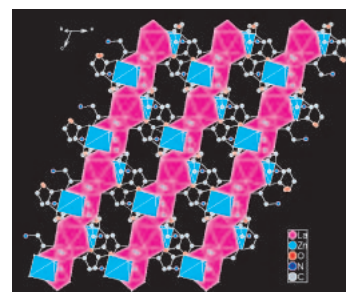
444 **An Improved Synthesis of Chacotriose**



Vincent Lequart, Gérard Goethals, Joseph Banoub, Pierre Villa, and Patrick Martin

446 **Syntheses and Structure of a Novel Layered Lanthanide-Zinc Coordination Polymer:  $[\text{LaZn}(\text{HIDA})(\text{IDA})_2 \cdot 0.5\text{H}_2\text{O}]_n$**

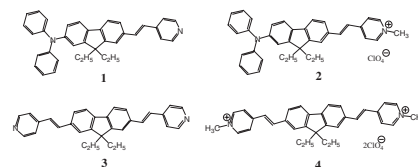
La ions are lined through sharing the O atoms of IDA ligands to form a 1-D zig-zag chain, and octahedron-coordinated Zn ions are beside the 1-D chain, alternately. And then HIDA ligand showing an unusual protonated helix bridging mode, link the 1-D zig-zag inorganic chain into 2-D layered structure.



Hongbin Xu, Yahui Zhao, Zhongmin Su, Guanghua Li, Yue Ma, Kuizhan Shao, Dongxia Zhu, Hengjun Zhang, and Shumei Yue

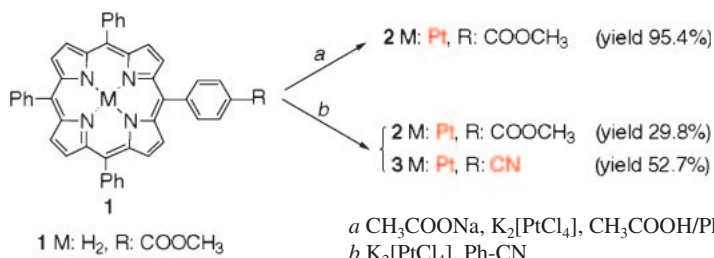
448 **Two-Photon Absorption Cross-Sections of Fluorene Derivatives with Cationic Substituents**

Fluorene derivatives with an ionic substituent (**2** and **4**) were newly synthesized and their two-photon absorption (TPA) cross-sections were examined. As a result, much larger TPA cross-sections were observed for compounds **2** and **4** than those observed for the compounds **1** and **3**.



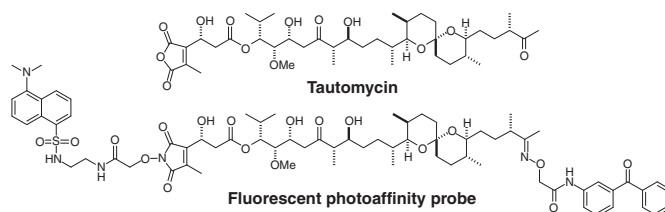
Jun Kawamata, Masaharu Akiba, Takeharu Tani, Akinori Harada, and Yoshio Inagaki

## 450 Unprecedented Pendant Group Exchange of a Porphyrinato Platinum(II) in Benzonitrile



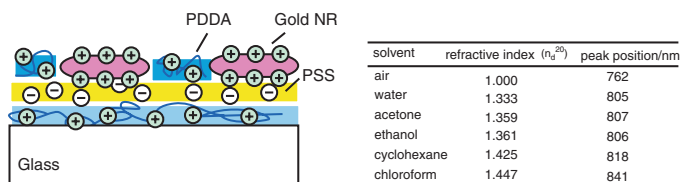
Naoko Araki, Makoto Obata, Akio Ichimura, Yuji Mikata, and Shigenobu Yano

## 452 Synthesis and Physical Nature of Fluorescent Photoaffinity Probe for the Bioorganic Studies on Tautomycin, a Protein Phosphatase Type 1 Selective Inhibitor



Masakuni Kurono and Minoru Isobe

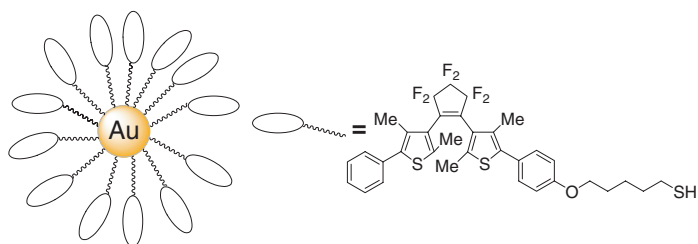
## 454 Immobilization of Gold Nanorods on the Glass Substrate by the Electrostatic Interactions for Localized Plasmon Sensing



The outermost PDDA layer was effective to prevent the lateral diffusion of gold NRs on the PSS layer. The longitudinal SP band of the immobilized gold NRs without substantial aggregation could sense the refractive index of the surrounding medium.

Yasuro Niidome, Hironobu Takahashi, Shinji Urakawa, Koji Nishioka, and Sunao Yamada

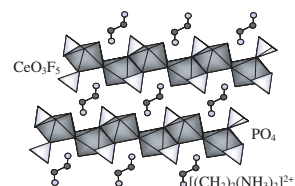
## 456 Photochromism of Diarylethene-capped Gold Nanoparticles



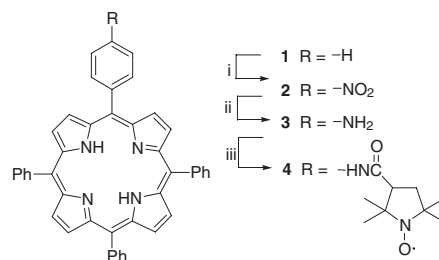
Kenji Matsuda, Masumi Ikeda, and Masahiro Irie

458 Synthesis and Characterization of the First Organically Templated Layered Cerium Phosphate Fluoride: [(CH<sub>2</sub>)<sub>2</sub>(NH<sub>3</sub>)<sub>2</sub>]<sub>0.5</sub>·[Ce<sup>IV</sup>F<sub>3</sub>(HPO<sub>4</sub>)]

By careful control of the reaction conditions, especially organic amine and system acidity, the first organically templated layered cerium phosphate fluoride has been hydrothermally synthesized. Its unique layered structure is based on a network of novel polyhedral CeO<sub>3</sub>F<sub>3</sub> and tetrahedral PO<sub>4</sub>. The structure consists of macroanionic [Ce<sup>IV</sup>F<sub>3</sub>(HPO<sub>4</sub>)] sheets separated by diprotonated ethylenediammonium cations.

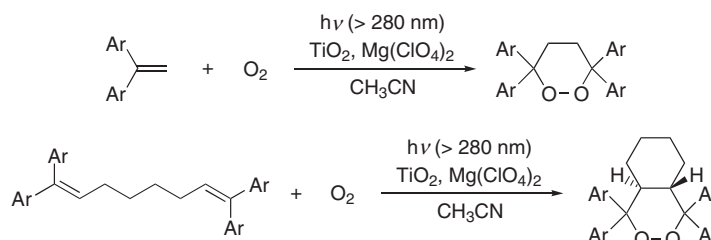


Ranbo Yu, Dan Wang, Shintaro Ishiwata, Takashi Saito, Masaki Azuma, Mikio Takano, Yunfa Chen, and Jinghai Li

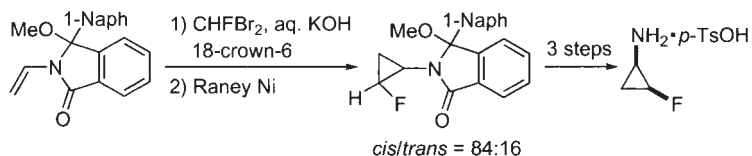
460 **Synthesis and Photocytotoxicity of Nitroxyl Radical-substituted Porphyrin**

Jian Wu, Weimin Shi, and Di Wu

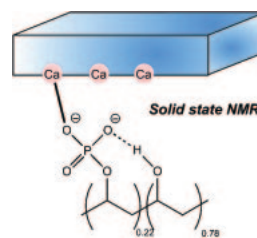
mono-nitroxyl radical-substituted tetraphenylporphyrin

462 **Synthesis of 3,3,6,6-Tetraaryl-1,2-Dioxanes via TiO<sub>2</sub>-catalyzed Photooxygenation of 1,1-Diarylethenes in the Presence of Mg(ClO<sub>4</sub>)<sub>2</sub>**

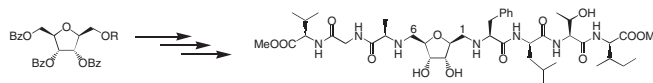
Hajime Maeda, Hisayuki Miyamoto, and Kazuhiko Mizuno

464 **Synthesis of *cis*-2-Fluorocyclopropylamine by Stereoselective Cyclopropanation Under Phase-transfer Conditions**

Jun-ichi Matsuo, Yu-ichirou Tani, and Yu-ichirou Hayakawa

466 **Solid State <sup>31</sup>P MAS NMR Detection of Hydrogen-bonded Phosphate Polymer in Calcium-Phosphate Composites**

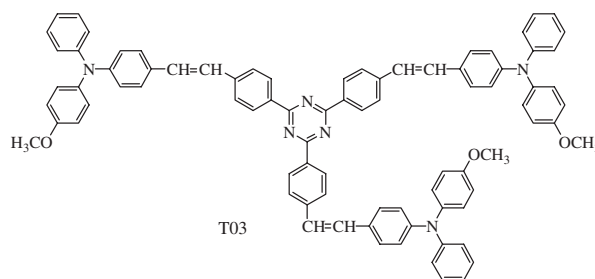
Akira Onoda, Mototsugu Doi, Kazuyuki Takahashi, Taka-aki Okamura, Hitoshi Yamamoto, and Norikazu Ueyama

468 **Novel Reversed Chain Modified Oligopeptides via Sequential  $\alpha$ -N-Mitsunobu Condensation of a Functionalized C-glycoside**

John J. Turner, Friso D. Sikkema, Kees Erkelens, Gijs A. van der Marel, Herman S. Overkleeft, Jacques H. van Boom, and Mark Overhand

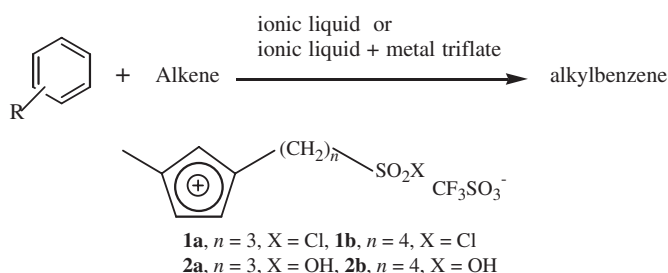
470 **Enhanced Two-photon Properties of Tri-branched Styryl Derivatives Based on 1,3,5-Triazine**

Fanshun Meng, Bo Li, Shixiong Qian, Kongchang Chen, and He Tian



472 **Novel Acidic Ionic Liquids Catalytic Systems for Friedel-Crafts Alkylation of Aromatic Compounds with Alkenes**

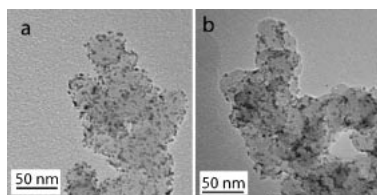
Kun Qiao and Chiaki Yokoyama



474 **Microwave Polyol Synthesis and Characterizations of Carbon-supported Pt and Ru Nanoparticles**

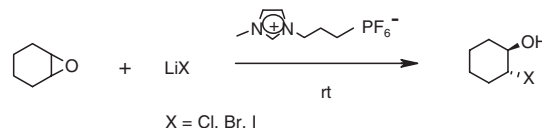
Weixiang Chen, Jie Zhao, Jim Yang Lee, and Zhaolin Liu

Carbon-supported Pt and Ru nanoparticles were prepared by microwave polyol process. Pt and Ru particles prepared as such have uniform shapes and sizes, and well dispersed on the carbon surface.



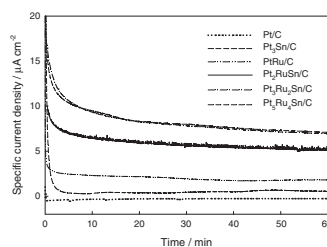
476 **Green Protocol for the Synthesis of vicinal-Halohydrins from Oxiranes Using the [Bmim]PF<sub>6</sub>/LiX Reagent System**

J. S. Yadav, B. V. S. Reddy, Ch. Srinivas Reddy, and K. Rajasekhar



478 **Methanol Electrooxidation on Carbon-Supported Pt<sub>3</sub>Ru<sub>2</sub>Sn Ternary Catalyst**

Taeyoon Kim, Masashi Takahashi, Masayuki Nagai, and Koichi Kobayashi



Methanol oxidation currents with time on the carbon-supported Pt alloy catalysts at room temperature (potential: 0.45V vs. RHE, electrolyte: 0.1M H<sub>2</sub>SO<sub>4</sub>, 0.5M methanol, loading weight of catalyst: based on same 21 μg<sub>Pt</sub>/cm<sup>2</sup>).